

# A fundamental explanation of softening

Jan G.M. van Mier

*ETH Zurich, Institute for Building Materials, 8093 Zurich, Switzerland*

**ABSTRACT:** Softening of concrete must be considered as the stage where the material breaks down catastrophically. For plain concrete and cement it can be shown that a macroscopic crack develops, most generally in asymmetric mode. This is caused by the heterogeneous material structure of said materials. The macrocrack growth is affected by boundary conditions and specimen/structure size. The phenomena can be realistically described by means of a bridged crack model based on LFM principles. Both for tension and compression the observed crack sequence from micro-cracking in the pre-peak regime to localized crack growth in the post-peak regime can be shown, with the exception that the macrocrack growth is in mode II in compression rather than in mode I. In both cases boundary effects are important and cannot be neglected. The paper shows that the unrestricted use of softening curves as material property is not allowed; rather every structure will have its own specific softening curve.

## 1 INTRODUCTION

Concrete has a quite large-scale microstructure (material structure), which makes an approach via continuum mechanics rather complicated. Especially for analyzing small structures and/or laboratory-size specimens the heterogeneity caused by the large aggregates cannot be ignored and averaging is difficult if not impossible. Nevertheless, continuum-based approaches appear to be favored in the engineering community. An enormous variety of models and theories has been proposed over the past decades trying to capture the highly non-linear material behaviour of concrete including the softening part of the stress-deformation curve in a continuum-mechanics framework. One can question whether such approaches are realistic. Averaging seems appropriate when elastic properties of cement and concrete are considered, provided of course that experimental information is obtained from specimens larger than the Representative Volume for these materials. The Representative Volume Element (RVE) for concrete can be quite large, namely at least larger than 8 times the maximum aggregate size  $d_{max}$  in the case of normal concrete with strong, stiff natural aggregate particles (Van Mier 1999). Normally an RVE of 3-5 times the maximum aggregate size would suffice, but considering environmental effects like drying shrinkage, differential hydration and the like, experiments suggest that a value of  $8d_{max}$  for concrete is more realistic.

When it comes to fracture it is highly questionable if a continuum-based approach should be considered at all. Starting from the beginning of load-

ing, small tensile microcracks develop within the concrete micro-structure (irrespective of the fact whether the external loading is tensile or compressive). The relation between microcracking and the shape of the stress-strain curve in compression was first pointed out by Hsu et al. (1963). The microcracks gradually increase in size until one or several cracks become so large that catastrophic failure occurs and the specimen/structure under consideration breaks into two or several large parts. Typically these residual parts have a characteristic dimension equal to the characteristic structure dimension  $\ell$  (for example thickness). Note that in this introduction as in the sequel of this paper the terms 'structure' and 'laboratory specimen' are treated as synonyms. A laboratory-scale specimen (characteristic length  $\ell$  in the order of 100 mm) behaves when it fractures as a 'small-scale structure', since, as will become clear, specimen size and boundary conditions play an important role. One of the most visible effects of the growth of macrocracks is localization of deformations, which led Hillerborg, Modéer and Petersson to develop the Fictitious Crack Model in 1976. The Fictitious Crack Model (FCM) is similar to the cohesive crack models (CCM) considered earlier by Dugdale and Barenblatt: a non-linear fracture process zone is assumed to precede the growth of a stress-free macrocrack. The crack length that enters into the formulation is the stress-free crack length plus the length of the cohesive zone (or process zone). One significant difference exists between the FCM for concrete and the CCM, which was originally developed for describing fracture in ductile metals. In CCM the size of the fracture process zone

(or rather plastic zone) is assumed to extend over a very short length in front of the stress-free macro-crack (Barenblatt 1962, Lawn 1993). The typical dimension is a few grain sizes in metals, corresponding to several micrometers.

In materials like concrete there is still no agreement about the actual size of the fracture process zone (e.g. Mindess (1991) who explored the idea of a ‘cloud of microcracks in front of a stress-free macro-crack, or Van Mier (1991) who put forward a completely different interpretation based on bridging in the wake of the crack-tip), but many would agree that under some circumstances it can be larger than the structures’ characteristic length  $\ell$ . It appears that for materials like concrete (and also rock and ice) the fracture process zone becomes thus a global parameter rather than the local effect as considered in the CCM. The consequences are important. If the fracture process zone size becomes equal or larger than the structure characteristic length, size-effects and boundary condition effects will start to play a role, as a matter of fact already before a macroscopic (stress-free) crack develops.

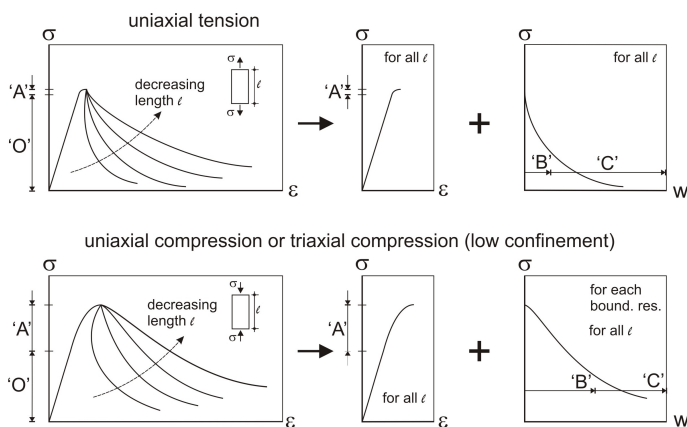


Figure 1. (a) The Fictitious Crack Model developed by Hillerborg, Modeer & Petersson (1976) separates the stress-strain curve for concrete in tension into two parts: a pre-peak stress-strain curve and a post-peak stress-crack opening diagram. (b) Uniaxial compression experiments by Van Mier (1984) showed that the same separation can be applied and leads to a unique stress-post-peak displacement curve. Later the localization effect in compression was shown to be independent on the type of loading platen used (frictionless or un-restrained, or restrained) by Van Vliet & Van Mier (1996). Four stages are distinguished in the tensile and compressive fracture process: ‘O’ (elastic), ‘A’ (microcracking, stable), ‘B’ (macro-cracking, inherently ‘unstable), and ‘C’ (bridging, which must be interpreted as coulomb friction in compression). Note that the tensile and compressive diagrams are not drawn to scale.

The main question addressed in this paper is how the fracture process zone should be interpreted, and how it should be considered in a fracture mechanics-based analysis. In the discussion that follows, uniaxial tensile and uniaxial compressive loading lead to the same result. In 1984 Van Mier showed in a series of uniaxial compression experiments that localization occurs in the same way as under uniaxial ten-

sion. The stress-strain curve in compression becomes meaningless in the softening regime; rather a stress-displacement curve must be adopted to describe the behaviour during softening independent of structure length. Thus, as sketched in Figure 1, the ‘Fictitious’ approach can be translated directly to compression.

Although the ‘fictitious’ crack model seems appealing and correct, it is only superficially so since the effect of stress-concentration, the material heterogeneity and the ensuing non-uniform crack process is completely missed. In order to simulate non-uniform crack-opening as observed in uniaxial tension tests (Van Mier 1997), a defect must be included. The defect may be a notch, an element with a deviating stiffness, or an element with deviating (usually, lower) strength, all under the assumption that the simulation is carried out with the finite element method, which appears to be the only means to apply the FCM. For FCM interface elements are needed; the crack-band model (Bažant & Oh 1983) can use the same type of element for the entire structure and the crack-path must not necessarily be known in advance, although new difficulties arise for curved cracks. We will not delve into those matters here.

In this paper an approach based on linear-elastic fracture mechanics is suggested that allows computing the softening behaviour of a structure as a crack growth phenomenon. In this approach a crack (and also a micro-crack) is a displacement jump in an otherwise elastic continuum; no tensile stress transfer is possible perpendicular to the crack surfaces. Stress-crack-opening diagrams can be retrieved using well-known equations from LEFM. Since crack-face bridging plays a role in tensile fracture of plain concrete and plain cement (i.e. the main crack is not continuous but contains small overlaps), and to a larger extent in fibre reinforced concrete (in the form of fibre bridging), and since this is only mobilized after the main localized crack starts to propagate, a different bridging stress must be applied. Balancing the stress-intensity from the mechanical loading with the stress-intensity of the bridging stress leads to different behaviour directly after peak. In other words the stability of the crack is affected by the bridging stress since it directly affects the stress-intensity that drives the crack. In compression the same approach may be used, except that now mode II is considered rather than mode I. The LEFM-based model has an advantage, namely that geometry and boundary condition effects are directly incorporated via the weight function. Disadvantage is that these weight functions are mostly known for single-crack problems only, and can be mathematically quite demanding. On the other hand, since softening is a ‘single-crack phenomenon’, the LEFM approach is a viable choice non-the-less.

## 2 FRACTURE PROCESS IN CONCRETE

### 2.1 Uniaxial tension

The stable displacement-controlled experiments by Evans & Marathe (1968) suggested that microcracking starts before the maximum tensile stress is reached. This statement is confirmed by acoustic emission measurement, for example Wissing (1988). The localized macrocrack, which leads to catastrophic rupture, starts to grow around maximum load. This can, for instance be shown by means of photoelasticity (coating glued on the surface of a concrete specimen, Van Mier & Nooru-Mohamed 1990), Moiré-interferometry (for example Raiss et al. 1989), vacuum impregnation with super-fluid epoxy or dye (Van Mier 1991), or X-ray tomography (Trtik et al 2007). The main crack is not continuous but contains numerous crack-face bridges where stress-transfer is still possible. This crack-face-bridging is assumed to take place in the wake of the main crack tip, and has also been observed in other materials, like ceramics (see for example in Lawn 1993). Thus, including the linear-elastic regime, four stages are recognized. In Figure 1a these are labeled ‘O’ (elastic), ‘A’ (stable micro-cracking), ‘B’ (macrocracking, which is inherently un-stable, see Van Mier & Shi 2002) and ‘C’ (bridging).

### 2.2 Compression (low confinement)

In compression the failure sequence is the same. After an initially linear regime ‘O’ (Figure 1b), stable microcracking is observed. The microcracking is usually thought to start at a stress-level of  $0.30f_c$ , but when very accurate strain measurements are made the  $\sigma$ - $\varepsilon$  curve appears to be non-linear from the very beginning. This may in part be caused by the closure of small voids and pre-existing (shrinkage) cracks at very small compressive loads. The microcracking in compression is very stable: the cracks are mostly oriented parallel to the loading direction and the load must be increased in order to propagate the small cracks. In addition, like in tension, the heterogeneous microstructure of concrete provides ample opportunity for crack-arrest. Often the definition of a ‘microcrack’ is raised as an issue. In principle, when the stability of a crack is considered one could define a ‘microcrack’ as one with a positive geometry, i.e. the stress-intensity increases when the crack grows. The absolute size-definition is then irrelevant. For example in fibre concrete, long stable cracks may be observed (referred to as ‘multiple cracking’), but since the fibres in the material tend to arrest them, they may also be considered as microcracks (see also Section 4). Hsu et al. (1963) showed the growth of microcracks in cylinders subjected to compression by means of a dye-technique. The same

techniques mentioned above for tensile cracking can be used in compression as well. Notably is that for stress-levels up till approximately 70-75% of maximum stress the volume of the specimen decreases, whereas after that an increase is observed, indicating that the cracks are opening. At or just beyond peak an ‘unstable’ macrocrack propagates through the compressed specimen leading to catastrophic failure if not the test is conducted in displacement control. Note that localization of deformations occurs in compression (Van Mier (1984)). Thus, again four stages can be distinguished, and they are the same as those mentioned for tensile fracture (compare Figures 1a and 1b). With that a unified approach for tension and compression appears to be within reach. Note that the last regime ‘C’ (bridging) must in the compressive case be interpreted as Coulomb friction in an inclined macrocrack, see Van Mier (2009).

## 3 LEFM SOLUTION: THE TENSILE CASE

In this paragraph we consider tensile fracture only; compression can be dealt with identically, using however the expressions for mode II fracture instead of those for mode I. In LEFM, for the stresses at the tip of a slit-like crack in a homogeneous isotropic elastic-brittle material the following equations apply,

$$\begin{Bmatrix} \sigma_{xx} \\ \sigma_{yy} \\ \sigma_{xy} \end{Bmatrix} = \frac{K_I}{\sqrt{2\pi r}} \begin{Bmatrix} \cos \frac{\theta}{2} \left[ 1 - \sin \frac{\theta}{2} \sin \frac{3\theta}{2} \right] \\ \cos \frac{\theta}{2} \left[ 1 + \sin \frac{\theta}{2} \sin \frac{3\theta}{2} \right] \\ \sin \frac{\theta}{2} \cos \frac{\theta}{2} \cos \frac{3\theta}{2} \end{Bmatrix}$$

$\sigma_{zz} = 0$  for plane stress, and  $\sigma_{zz} = \nu(\sigma_{xx} + \sigma_{yy})$  for plane strain.  $K_I$  is the mode I (tensile) stress-intensity factor, which depends on the external applied tensile stress  $\sigma$ , the half-crack length  $a$  and a weight-function  $f(a/W)$ . The weight function depends on the actual specimen geometry and boundary conditions. In short, the crack-tip stresses can be written as

$$\sigma_{ij} = \frac{K_I}{\sqrt{2\pi r}} f_{ij}(\theta)$$

For the displacements the expressions are:

$$\begin{Bmatrix} u_x \\ u_y \end{Bmatrix} = \frac{K_I}{2E} \sqrt{\frac{r}{2\pi}} \begin{Bmatrix} (1+\nu) \left[ (2\kappa-1) \cos \frac{\theta}{2} - \cos \frac{3\theta}{2} \right] \\ (1+\nu) \left[ (2\kappa+1) \sin \frac{\theta}{2} - \sin \frac{3\theta}{2} \right] \end{Bmatrix}$$

and  $u_z = -\frac{\nu z}{E}(\sigma_{xx} + \sigma_{yy})$  for plane stress and  $u_z = 0$  for plane strain.  $\kappa$  is the bulk modulus for plane

stress  $((3-\nu)/(1+\nu))$  or for plane strain  $(3-4\nu)$ . In short the displacements are written as:

$$u_i = \frac{K_I}{2E} \sqrt{\frac{r}{2\pi}} f_i(\theta)$$

Under pure mode I loading (tension), Lawn (1993) shows that the crack-opening displacement at the tip (in the direction of loading, i.e. the  $y$ -direction) is parabolic:

$$u(r) = \frac{K_I}{E} \sqrt{\frac{8r}{\pi}}, \text{ for } r > 0, \text{ and for plane stress.}$$

This result can be obtained by substituting  $\theta = \pm \pi$  in the expression for  $u_y$ . For plane strain,  $E$  must be substituted by  $E/(1-\nu^2)$ .

For mode II and mode III the expressions are slightly different, and can be found in various textbooks (e.g. Suresh (1991), Lawn (1993)).

As mentioned, the  $K$ -factor, the stress intensity factor, depends on the outer boundary conditions of the specimen/structure, whereas the remaining factors depend only on the local coordinates at the crack-tip. For every structure the  $K$ -factor must be determined again. This can be done numerically, or for a number of special cases where a closed-form solution has been derived, via handbooks, e.g. Tada et al. (1973).

Now, a crack is assumed to start propagating when  $K_I$  exceeds a critical value denoted by  $K_{Ic}$ . The critical value can be determined from experiments at peak stress, provided that a good measure for the initial crack length is available. The critical stress intensity factor is assumed to be a material constant. The critical crack is assumed to grow during the post-peak regime (stage 'A') and is the actual start of the softening stages ('B' and 'C'). The effective carrying capacity of the specimen/structure decreases as the critical crack grows. Bridging may have a positive effect in the sense that the load-decrease is slower since some load can still be applied by the bridges connecting the two crack faces. Examples of crack face bridging are 'aggregate bridging', which is usually observed in plain concrete (Van Mier (1991)), or fibre bridging in fibre reinforced composites, see for example Rieger & Van Mier (2009).

The load-decrease due to a growing mode I crack can be written as

$$\frac{\sigma_1}{\sigma_0} = \frac{f(\xi_0)}{f(\xi_1)} \cdot \sqrt{\frac{\xi_0}{\xi_1}}$$

where the relative crack length is denoted  $\xi_i = a_i/W$  ( $i \geq 0$ ), and  $W$  is the specimen width, Van Mier

(1991). The shape of the stress-relative crack length curve depends on the initial crack length  $\xi_0$ , and most importantly, on the boundary conditions and the geometry of the structure (weight function  $f$ ). Figure 2 shows a comparison between specimens loaded in tension between rotating (Fig. 2a) and fixed loading platens (Fig. 2b). Experiments show exactly this distinct post-peak (softening) behaviour.

The relative crack-length can be replaced by the crack-opening displacement in Figure 2: this will not change the shape of the diagrams. Using the expression for  $u$  (see above), one can easily show that in the post-peak regime

$$\frac{u_1}{u_0} = \sqrt{\frac{a_1}{a_0}}$$

Note that  $u_1$  is the displacement normal to the crack in the post-peak regime, whereas  $u_0$  denotes the displacement at peak load. An important assumption in the above analysis is that the stress-intensity is constant and equal to the critical value  $K_{Ic}$  during the growth process in the post-peak regime.

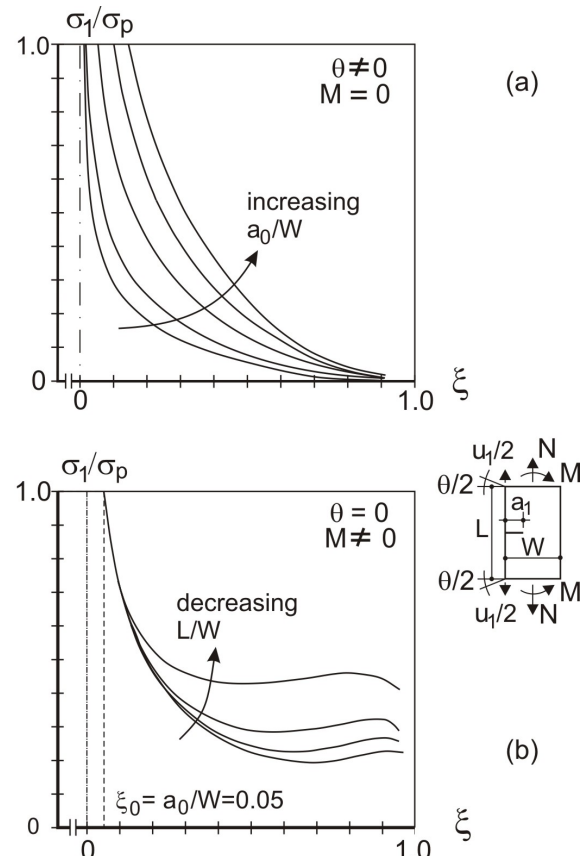


Figure 2. Decrease of load carrying capacity with increasing relative crack length  $\xi$ , for a single-edge-notched plate loaded in uniaxial tension: (a) freely rotating platens ( $\theta \neq 0$ ), and (b) fixed loading platens ( $\theta = 0$ ), after Van Mier (1991).

Moreover, an initial crack, with length  $a_0$ , needs to be present in the material. It seems likely that this is the first microcrack in the pre-peak regime that

becomes unstable. How large such a microcrack would be depends on the microstructure of the concrete mixture. From micro-mechanics analysis it follows that the pre-peak microcrack process is, for example, influenced by the amount and size of the aggregates that are used, see for example Prado & Van Mier (2003).

For compressive loading all equations must be replaced by those for mode II; the direction of the mode II crack is determined by the type of material and the amount of boundary friction (restraint) between loading platen and specimen, see Van Mier (2009). Note that plane-stress conditions are assumed here. In reality fracture of concrete must usually be treated as a plane-strain problem, especially when laboratory-scale specimens are analyzed. In that case prismatic specimens often show crack initiation in a corner, which could be analyzed by considering a 3D-elliptic corner crack. In cylindrical shaped specimens the stress-concentration from corners is missing, and just a planar crack is observed in compression. What will happen for each individual specimen is hard to say since crack initiation depends on local variations in material structure and material strength and the imposed irregularities from specimen geometry (for example prisms vs. cylinders) and boundary restraint.

#### 4 THE ROLE OF BRIDGING

What has not been included in the above analysis is the effect of bridging (for tension) or Coulomb friction in the crack (for compression). Again, limiting ourselves to mode I fracture, the crack must be considered as not being stress-free, but rather a uniformly distributed bridging stress counter-acts the stress-intensity from the externally applied load as sketched in Figure 3.

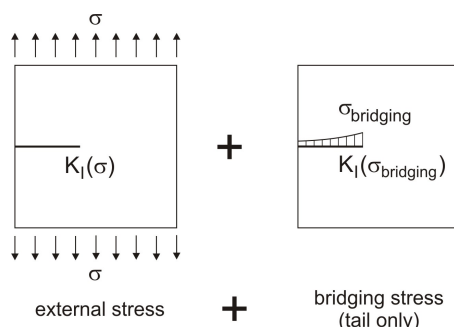


Figure 3. Superposition principle applied to a bridged macrocrack in tension: (a) stress-free macrocrack in a specimen/structure subjected to external tension, (b) bridging stress over the slit-like crack due to crack face bridging. Ideally the bridging stress distribution follows from micromechanical considerations, for example on aggregate pullout, crack-overlaps or fibre pullout.

A bridged macrocrack takes a shape like that shown in Figure 4. Crack overlaps, and sometimes

crack branches allow for local stress-transfer. The crack overlaps have been shown in the past at many different scales (from [ $\mu\text{m}$ ] to [ $\text{km}$ ]), in a variety of (heterogeneous) materials. From simple lattice analysis the bridging mechanism evolves automatically, and in Prado & Van Mier (2003) the stress-transfer due to bridging has been visualized, as well as other stages in the fracture process.

Again, returning to the LEFM-approach, for straight cracks one may apply the superposition principle, and simply one should consider

$$K_I(\text{tot}) = K_I(\sigma) + K_I(\sigma_{\text{bridging}})$$

The stress-intensity from external load is counter-acted by the stress-intensity from a slit-like crack with bridging stress (negative internal pressure). If the number of crack overlaps is sufficiently large, one may assume a continuous bridging stress over the crack length. If the bridging stress increases, so that  $-K_I(\sigma_{\text{bridging}}) > K_I(\sigma)$ , the crack stops to grow. In the example of Figure 2b something similar happened: a bending moment develops with increasing  $\xi$  due to the increasingly eccentric loading when the loading platens are kept parallel (fixed). Eventually the moment is large enough to arrest the crack completely.

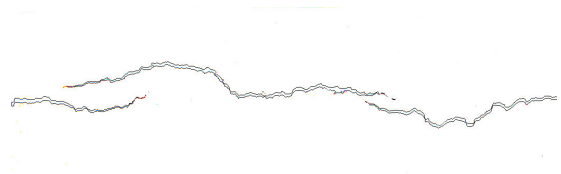


Figure 4. Example of bridging through crack-overlaps: this crack-mechanism has been demonstrated at various scales from [ $\mu\text{m}$ ] to [ $\text{km}$ ]. The tensile loading direction is vertical.

#### 5 RAMIFICATION TO OTHER STRUCTURES AND SIZE EFFECT

The consequence of the above explanation is that every structure has its own distinct softening behaviour. This is nothing new when one considers that every ‘material experiment’ will lead to a different strength value. For concrete compare, for example, the difference in ‘bending tensile strength’, ‘splitting tensile strength’ and ‘uniaxial (or direct) tensile strength’. Bending, splitting or direct tension all lead to different values for the presumed ‘tensile strength of concrete’, and the debate of how to translate one into the other is an ongoing activity, which is likely never to be solved. Returning to the case for softening, perhaps for some classes of more-or-less identical cracking behaviour a softening rule could be defined, but the tensile example shows that one should be careful (Fig. 2). On the other hand, the situation for structural analysis may now focus on the real is-

sue, namely the development of micro-cracks in stage 'A', as defined in Figure 1. The real problem is to find out when the microcracks tend to become unstable, i.e. when the structure of the material (think of aggregate particles and/or fibres in concrete) and the specimen geometry and boundary conditions are not capable anymore to arrest cracks. As soon as this point has been established, the strength of the structure is known, and the next important step is to determine whether the propagation of the main localized macro-crack is fast or slow (think about possible positive effects of bridging by aggregates and/or fibres, or the effect of external confinement in the case of compression, see Van Mier (2009)).

There are consequences for handling size effects as well. Different concretes containing different amounts of coarse aggregates are shown to lead to distinct stage 'A' behaviour, see for example the analyses presented in Prado & Van Mier (2003). Here a detailed analysis of the pre-peak microcrack stage is needed in order to predict the peak strength. Obviously when the interplay of the various material phases in concrete, aggregate, matrix and interfacial transition zones leads to delayed pre-peak (stage 'A') cracking, a higher load is achieved, whereas when the interplay is not effective the first crack will become immediately un-stable. Such differences lead to different size effects, and the type of material must somehow be taken into account. The best way will be detailed analyses of the fracture process, as for example attempted by Man (2009).

## 6 CONCLUSION

The main conclusion is that softening is a structural property and not a material property. Consequently each structure (or laboratory-scale test specimen) will have its own distinct softening curve. The fracture process described via the LEFM-equations can be automatically retrieved from micromechanics-based approaches that include the material structure and a simple meso-level fracture criterion. The amount of detail is of course much larger in micromechanics models, which are elegant and simple, but both the interface-type models (for example, one of the earlier 'numerical concrete' models by Roelfstra et al. (1985)), and particle- or lattice-type approaches (Schlangen & Van Mier 1992, Lilliu & Van Mier 2003, Bolander et al. 1996) require substantial computational effort. Nevertheless, considering progress made over the past two decades the micromechanics approach will eventually completely overtake the mathematically-demanding LEFM method described in this paper. Continuum-based fracture mechanics approaches are ineffective in describing the fracture process, and are therefore not

considered very useful and will likely become obsolete over time.

This paper is rather philosophical, but reflection is critically needed. As an experimentalist I believe it would bear fruit if models are based on the actually observed fracture mechanisms and contain well defined parameters. The fracture process described in this paper is well documented by experiment, and should form the basis for any further development.

## REFERENCES

- Barenblatt, G.I. 1962. The mathematical theory of equilibrium of cracks in brittle fracture. *Advances in Applied Mechanics* 7: 55-129.
- Bažant, Z.P. & Oh, B.-H. 1983. Crack band theory for fracture of concrete. *Mater.Struct. (RILEM)* 16: 155-177.
- Bolander, J.E. Shiraishi, T. & Isagawa, Y. 1996. An adaptive procedure for fracture simulation in extensive lattice networks. *Eng.Fract.Mech.* 54: 325-334.
- Dugdale, D.S. 1960. Yielding of steel sheets containing slits. *Journal Mechanics of Physics and Solids* 8: 100-108.
- Evans, R.H. and Marathe, M.S. 1968, Micro-cracking and Stress-Strain Curves for Concrete in Tension, *Mater.Struct. (RILEM)*, 1(1), 61-64.
- Hillerborg, A. Modeer, M. & Petersson, P.-E. (1976), Analysis of crack formation and crack growth in concrete by means of fracture mechanics and finite elements, *Cem.Conc.Res.* 6(6): 773-782.
- Hsu, T.T.C. Slate, F.O. Sturman, G.M. & Winter, G. 1963. Microcracking of plain concrete and the shape of the stress-strain curve. *ACI Journal* 60(14): 209-224.
- Lawn, B. 1993. *Fracture of Brittle Solids*. Cambridge: Cambridge University Press (2nd edition).
- Lilliu, G. & Van Mier, J.G.M. 2003. 3D lattice type fracture model for concrete, *Eng.Fract.Mech.* 70(7/8): 927-942.
- Man, H.-K. 2009. *Analysis of 3D Scale and Size Effects in Concrete*, PhD-thesis, ETH Zurich.
- Mindess, S. 1991. Fracture process zone detection, In S.P. Shah and A. Carpinteri (eds.), *Fracture Mechanics Test Methods for Concrete*: 231-261. London/New York: Chapman & Hall.
- Prado, E. & Van Mier, J.G.M. 2003. Effect of particle structure on mode I fracture process in concrete, *Eng.Fract.Mech.*, 70(14): 1793-1807.
- Raiss M.E., Dougill J.W. and Newman J.B. 1989. Observation of the development of fracture process zones in concrete, In S.P. Shah, S.E. Swartz and B. Barr (eds.), *Fracture of Concrete and Rock -Recent Developments*: 243-253. London/New York: Elsevier Applied Science.
- Rieger C. & Van Mier J.G.M. 2009. Pullout of microfibers from hardened cement paste, In G.P.A.G. van Zijl and W.P. Boshoff (eds.), *Advances in Cement-based Materials*, Taylor & Francis Group, London, UK, 67-73.
- Roelfstra P.E. Sadouki, H. & Wittmann, F.H. 1985. Le béton numérique. *Mater.Struct. (RILEM)*, 18: 327-335.
- Schlangen, E. & Van Mier, J.G.M. 1992. Experimental and numerical analysis of the micro-mechanisms of fracture of cement-based composites. *J.Cem.Conc.Comp.* 14(2): 105-118.
- Suresh, S. 1991. *Fatigue of Materials*. Cambridge: Cambridge University Press.
- Tada, H. Paris, P.C. & Irwin G.R. 1973. *The Stress Analysis of Cracks Handbook*. St. Louis: Del Research Corporation.

- Trtik P. Stähli P. Landis E.N. Stampanoni M. & Van Mier J.G.M. 2007. Micro-tensile testing and 3D imaging of hydrated Portland cement", In A. Carpinteri, P. Gambarova, G. Ferro & G. Plizzari (eds.), *Proc. 6<sup>th</sup> Int. Conf. on 'Fracture Mechanics of Concrete and Concrete Structures' (FraMCoS-VI)*: 1277-1282. London: Taylor & Francis Group/Balkema.
- Van Mier J.G.M. & Nooru-Mohamed, M.B. 1990. Geometrical and structural aspects of concrete fracture, *Eng. Fract. Mech.*, 35(4/5), 617-628.
- Van Mier, J.G.M. & Shi, C. 2002. Stability issues in uniaxial tensile tests on brittle disordered materials, *Int.J.Solids Struct.*, 39(13/14): 3359-3372.
- Van Mier, J.G.M. 1984. *Strain-Softening of Concrete under Multiaxial Loading Conditions*, PhD-thesis, Eindhoven University of Technology.
- Van Mier, J.G.M. 1991. Mode I fracture of concrete: discontinuous crack growth and crack interface grain bridging. *Cem. Conc. Res.* 21(1): 1-15.
- Van Mier, J.G.M. 1997. *Fracture Processes of Concrete*. Boca Raton (FL): CRC Press.
- Van Mier, J.G.M. 2001. Micro-structural effects on fracture scaling in concrete, rock and ice. In J.P. Dempsey & H.H. Shen (eds.), *Proc. IUTAM Symp. on 'Scaling Laws on Ice Mechanics and Ice Dynamics'*: 171-182. Dordrecht/ Boston/London: Kluwer Academic Publishers.
- Van Mier, J.G.M. 2009. Mode II crack localization in concrete loaded in compression, *J.Eng.Mech.(ASCE)*, 135(1): 1-8.
- Van Vliet, M.R.A. & Van Mier, J.G.M. 1996. Experimental investigation of concrete fracture under uniaxial compression. *Mech.Coh.Frict.Mater.* 1: 115-127.
- Wissing B. 1988. Acoustic emission of concrete, *MS thesis*, Delft University of Technology, Dept. of Civil Eng. (in Dutch).